Acetylation Preserves Retinal Ganglion Cell Structure and Function in a Chronic Model of Ocular Hypertension

Oday Alsarraf,[1] Jie Fan,[1] Mohammad Dahrouj,[1] C. James Chou,[2] Phillip W. Yates,[1] and Craig E. Crosson[1]

[1]Storm Eye Institute, Department of Ophthalmology, Medical University of South Carolina, Charleston, South Carolina, United States
[2]Departments of Pharmaceutical and Biomedical Sciences, Medical University of South Carolina, Charleston, South Carolina, United StatesStates

Correspondence: Jie Fan, Storm Eye Institute, Room 518, Medical University of South Carolina, 167 Ashley Avenue, Charleston, SC 29425, USA; fan@musc.edu.

Submitted: May 14, 2014
Accepted: October 16, 2014

Citation: Alsarraf O, Fan J, Dahrouj M, Chou CJ, Yates PW, Crosson CE. Acetylation preserves retinal ganglion cell structure and function in a chronic model of ocular hypertension. *Invest Ophthalmol Vis Sci*. 2014;55:7486–7493. DOI:10.1167/iovs.14-14792

Purpose. The current studies investigate if the histone deacetylase (HDAC) inhibitor, valproic acid (VPA), can limit retinal ganglion cell (RGC) degeneration in an ocular-hypertensive rat model.

Methods. Intraocular pressure (IOP) was elevated unilaterally in Brown Norway rats by hypertonic saline injection. Rats received either vehicle or VPA (100 mg/kg) treatment for 28 days. Retinal ganglion cell function and number were assessed by pattern electroretinogram (pERG) and retrograde FluoroGold labeling. Western blotting and a fluorescence assay were used for determination of histone H3 acetylation and HDAC activity, respectively, at 3-day, 1-week, and 2-week time points.

Results. Hypertonic saline injections increased IOPs by 7 to 14 mm Hg. In vehicle-treated animals, ocular hypertension resulted in a 29.1% and 39.4% decrease in pERG amplitudes at 2 and 4 weeks, respectively, and a 42.9% decrease in mean RGC density at 4 weeks. In comparison, VPA treatment yielded significant amplitude preservation at 2 and 4 weeks and showed significant RGC density preservation at 4 weeks. No significant difference in RGC densities or IOPs was measured between control eyes of vehicle- and VPA-treated rats. In ocular-hypertensive eyes, class I HDAC activity was significantly elevated within 1 week (13.3 ± 2.2%) and histone H3 acetylation was significantly reduced within 2 weeks following the induction of ocular hypertension.

Conclusions. Increase in HDAC activity is a relatively early retinal event induced by elevated IOP, and suppressing HDAC activity can protect RGCs from ocular-hypertensive stress. Together these data provide a basis for developing HDAC inhibitors for the treatment of optic neuropathies.

Keywords: retina, neuroprotection, acetylation, ocular hypertension

Glaucoma is a leading cause of blindness worldwide and affects 2% to 3% of Americans over the age of 40. The disease is clinically characterized by visual field loss, optic disc cupping, and retinal ganglion cell (RGC) degeneration, and is distinguished from other optic neuropathies by its slow progression usually over years to decades.[1] Although the primary risk factor for developing glaucoma is elevated intraocular pressure (IOP), it is estimated that between one-third and one-half of individuals with glaucoma have normal IOP.[2] Despite this evidence, the treatment of glaucomatous individuals continues to focus on reduction of IOP.[3] Studies have provided evidence that dysregulation of protein acetylation can play a central role in a variety of diseases, including some cancers, heart illnesses, and neurologic disorders. To date, two HDAC inhibitors, vorinostat (suberoylanilide hydroxamic acid [SAHA]) and romidepsin (Istodax, FK228), have both been clinically approved for the treatment of cutaneous T-cell lymphoma.[4] The intracellular acetylation-deacetylation status exists in equilibrium and is controlled by the opposing activity of histone acetyltransferases and histone deacetylases (HDACs).

In the eye, studies have demonstrated that increases in acetylation, via administration of HDAC inhibitors, can protect inner retinal neurons from severe forms of optic nerve damage including crush and ischemic injury.[5–8] Furthermore, evidence suggests that the aliphatic acid HDAC inhibitor valproic acid (VPA) attenuates glial microactivation in the brain.[9] Although VPA has multiple actions in addition to HDAC inhibition, studies from our laboratory have provided recent evidence that its neuroprotective actions in a model of ischemic retinal injury are due to its ability to inhibit HDAC activity.[10] This study utilized a rodent model of ocular-hypertensive injury to investigate how ocular hypertension alters retinal HDAC activity and protein acetylation and how the inhibition of HDACs affects retinal structure and function.

Materials and Methods

Animals

Adult male or female Brown Norway rats (3–5 months of age, 150–200 g; Charles River Laboratories, Inc., Wilmington, MA,

USA) were used in this study. Rats were maintained in an environmental cycle of 12 hours light and 12 hours dark. Animal handling and experimental protocols were performed in accordance with the ARVO Statement for the Use of Animals in Ophthalmic and Vision Research; and the study protocol was approved by the Animal Care and Use Committee at the Medical University of South Carolina. For neuroprotection studies, VPA (100 mg/kg) or vehicle (0.9% sodium chloride) was administered by intraperitoneal injection twice daily between 8:00 and 9:00 and again between 15:00 and 16:00 hours, starting on day 0 of ocular hypertension induction and ending on day 28 of the study. Nonhypertensive, contralateral eyes were used to evaluate the effects of VPA and vehicle administration on normal retinal structure and function.

Ocular Hypertension

Animals were allowed to acclimate to their surroundings 10 to 14 days prior to baseline IOP measurements and study initiation. On study day 0, rats were anesthetized with ketamine (75 mg/kg) and xylazine (8 mg/kg) (Ben Venue Laboratories, Bedford, OH, USA), and corneal analgesia was created by the application of proparacaine (0.5%, 5 μL; Akorn, Inc., Buffalo Grove, IL, USA). Body temperature was maintained at 37°C with a heating pad (Harvard Apparatus, Holliston, MA, USA). A pulled-glass micropipette attached to a syringe by polyethylene (PE-50) tubing (Becton Dickinson & Co., Sparks, MD, USA) was unilaterally inserted into a circumferential right limbal vein, and 50 μL 2 M hypertonic saline was injected into the limbal venous plexus as described by Morrison et al.[11] Prophylactic neomycin antibacterial ointment was applied to the site of injection of each eye to prevent infections. Intraocular pressure was recorded using a calibrated Tonolab tonometer (Colonial Medical Supply Co., Inc., Franconia, NH, USA) as the average of six consecutive measurements at each of the following time points relative to day 0 of ocular hypertension induction: −1, 3, 7, 10, 14, 21, and 28 days. Intraocular pressure was recorded as discrete readings as well as cumulative pressures that were calculated by integration of all prior IOP readings for each animal as described by McKinnon et al.[12] At day 10 following hypertonic saline injection, a minimum increase of 7 mm Hg was required for inclusion of the rats in the study. Forty rats were randomly divided into a vehicle group, receiving 0.9% sodium chloride twice daily, and a treatment group, receiving VPA (100 mg/kg) twice daily. Twelve rats were used for Western blotting and HDAC activity analysis at 3, 7, and 14 days after ocular hypertension initiation, and 20 rats were utilized for the entire 33-day study. The remaining 8 rats were used for immunohistochemistry and localization of acetylated histone H3.

Pattern Electroretinograms

Baseline pattern electroretinogram (pERG) recordings were conducted in bilateral eyes after stabilization of baseline IOPs 1 day prior to ocular hypertension induction, and then at 2 and 4 weeks following ocular hypertension initiation. For pERG measurements, rats were anesthetized with ketamine (75 mg/kg) and xylazine (8 mg/kg), and body temperature was maintained at 37°C with a heating pad. The pERG electrode was placed on the corneal surface and positioned to encompass the pupil without limiting the field of view. A normal saline drop was applied to keep the cornea moist during each recording. A visual stimulus was generated by black and white alternating contrast reversing bars (mean luminance, 50 cd/m^2; spatial frequency, 0.033 cyc/deg; contrast, 100%; and temporal frequency, 1 Hz) and was aligned with the projection of the pupil and visual axis at a distance of 11 cm from the center of the screen using the UTAS-2000 (LKC Technologies, Gaithersburg, MD, USA). Each pERG reading was recorded as an average of 300 sweeps at an interval of 1 second. Resulting pERG amplitudes were calculated as the difference between a peak and adjacent trough on the waveform.

Retrograde Labeling of Retinal Ganglion Cells

Rats were anesthetized with ketamine (75 mg/kg) and xylazine (8 mg/kg), and body temperature was maintained at 37°C with a heating pad. Retrograde labeling of RGCs was performed as described by Sawada et al.[13] Briefly, rats were immobilized in a stereotactic apparatus, and 3 μL 5% solution of hydroxystilbamidine (FluoroGold) (Fluorochrome, LLC, Denver, CO, USA) in PBS was injected into the superior colliculi bilaterally. More specifically, using a small drill, a 1/8-inch hole was made in the skull bilaterally 3 mm from midline, 6 mm from bregma, and 2 mm from lambda sutures. Subsequently, the needle of a Hamilton syringe (Hamilton, Reno, NV, USA) containing 3 μL FluoroGold dye was gently inserted 4 mm deep into the superior colliculi via the drilled holes, and dye was injected. The needle was left in the brain for 10 to 20 seconds and then gently removed. The skull hole was filled with bone wax 903 (Lukens Cat. No. 2007–05; World Precision Instruments, Inc., Sarasota, FL, USA). The skin was sutured; 0.5% erythromycin ophthalmic ointment (Bausch & Lomb, Inc., Tampa, FL, USA) was applied to the wound; and the animal was monitored closely until full recovery from anesthesia. Five days after FluoroGold injection, animals were euthanized and their eyes enucleated and fixed in 4% paraformaldehyde (PFA) for 24 hours at 4°C. After rinsing with PBS, each retina was detached from the eye cup and prepared as a flat mount with the vitreous surface facing upward. A suture was placed in the nasal side of the retina for orientation. Fluorescent RGCs were visualized under Zeiss microscopy (Carl Zeiss Imaging, Inc., Jena, Germany). Each retina was divided into four quadrants (superior and inferior, nasal and temporal), and images were obtained at 1.0 to 2.0 mm from the center of the optic disc in each quadrant. The size of counted area in each quadrant was 0.153 mm^2 (450 × 340 μm). Retinal ganglion cells were counted using ImageJ software (ImageJ; http://rsbweb.nih.gov/ij/; provided in the public domain by the U.S. National Institutes of Health, Bethesda, MD, USA)), and values were averaged in each quadrant of all eyes similarly. The automated RGC numbers generated by the ImageJ software were comparable when RGCs were counted manually by two operators in a masked fashion. No correction was made for the uptake of FluoroGold by microglia cells released by degenerating RGCs.[14] Hence cell counts may overestimate the number of RGCs in ocular-hypertensive eyes.

Western Blot Analysis

Western blot analysis was performed after homogenization of whole retinas in lysis buffer (50 mM Tris base; 10 mM EDTA; 0.5 mM sodium orthovanadate; 0.5% sodium deoxycholic acid; 1% Triton X-100) and protease inhibitors. Equivalent amounts of protein were loaded onto 10% SDS-polyacrylamide gels; proteins were separated by PAGE and transferred to nitrocellulose paper. The membranes were blocked in 5% nonfat dry milk followed by incubation for 24 hours at 4°C with appropriate primary antibodies selective for acetyl H3 (1:1000 dilution) (Cell Signaling Technologies, Beverly, MA, USA) and β-actin (1:1000 dilution) (Sigma-Aldrich Corp., St. Louis, MO, USA). After washing, membranes were incubated for 1 hour at room temperature with appropriate secondary

Investigative Ophthalmology & Visual Science

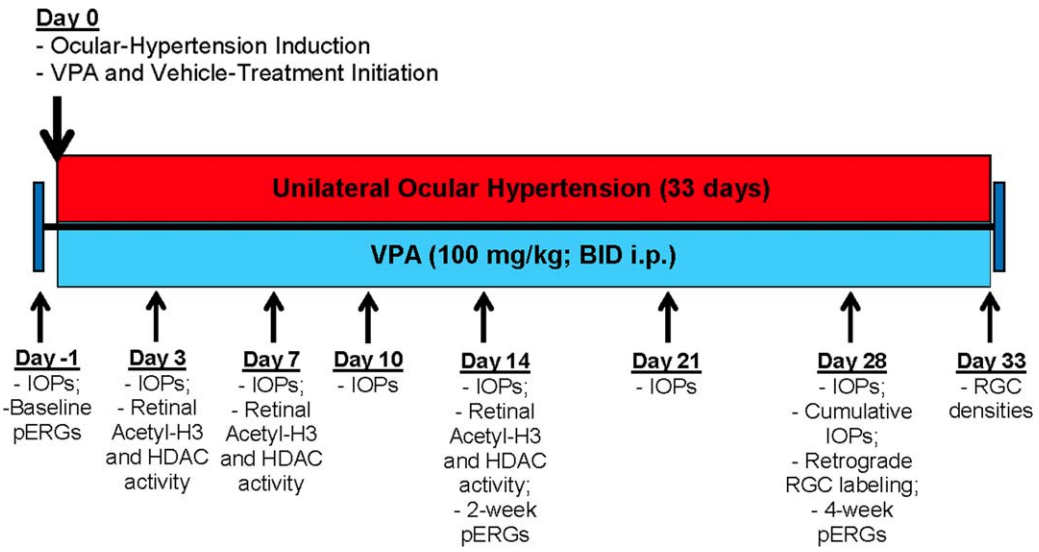

FIGURE 1. Schematic representation summarizing the key procedural aspects of the study. Each *arrow* corresponds to an important procedural time point, highlighting key experiments or measurements performed throughout the study. IOPs, intraocular pressure measurements; pERGs, pattern electroretinogram measurements; BID, twice daily; i.p., intraperitoneal; VPA, valproic acid.

antibodies (horseradish peroxidase [HRP] conjugated; 1:1000 dilution). Prestained molecular weight markers were run in parallel to identify the molecular weight of the proteins of interest. For chemiluminescent detection, the membranes were treated with enhanced chemiluminescence reagents, and the densitometric signal was monitored using a Bio-Rad Versadoc imaging system (Bio-Rad, Hercules, CA, USA).

HDAC Activity Assay

The deacetylase activities of class I and class II HDACs were measured by assaying enzyme activity using the peptidase, trypsin, and the fluorophore-conjugated synthetic substrate t-butoxyacetyl-lysine aminomethoxy-cumarin (Boc-Lys(Ac)-AMC) as previously described.[15] Briefly, lysates were diluted to a concentration of 1.0 μg/μL using standard HDAC buffer (50 mM Tris-Cl pH 8.0, 137 mM NaCl, 2.7 mM KCl, 1 mM $MgCl_2$, and 0.1 mg/mL bovine serum albumin) and incubated with the conjugated-fluorophore acetylated lysine substrate Boc-Lys(Ac)-AMC in 96-well nonbinding plates (Greiner Bio-One, Monroe, NC, USA) at room temperature for 2 hours. Baseline fluorescence was measured followed by treatment with the peptidase enzyme trypsin, freeing the fluorogenic 4-methyl-coumarin-7-amide (AMC). The amount of fluorogenic AMC generated was then measured using an excitation wavelength of 355 nm and emission wavelength of 460 nm with a standard fluorospectrometer. The substrate for class I in this assay is specific to HDAC1, 2, 3, and 6. The substrate for class II in this assay is specific to HDAC4, 5, 7, 8, 9, 10, and 11.

Immunohistochemistry

Selected eyes were fixed in 4% paraformaldehyde and embedded in paraffin, and retinal cross sections were cut at a thickness of 5 μm. Sections were blocked with 4% bovine serum albumin for 2 hours at room temperature, washed, and incubated with primary polyclonal acetyl-histone H3 antibody (1:500) (Cell Signaling Technologies) overnight at 4°C. Sections were then washed and incubated for 2 hours at room temperature with a FITC-labeled secondary antibody. For negative controls, staining with primary antibody was omitted, and sections were stained with only FITC-labeled secondary antibody. Retinal sections were observed and photographed by means of fluorescence microscopy (Axioplan-2; Zeiss, Maple Grove, MN, USA).

Statistical Analysis

For all experiments, data were expressed as mean ± SE. Statistical comparisons were made with Student's *t*-test for paired data or analysis of variance (ANOVA) using the Dunnett post test (GraphPad Software, Inc., San Diego, CA, USA); $P < 0.05$ was considered significant.

Figure 1 summarizes all the key procedural aspects of the study, indicating the time points of all experiments and interventions.

RESULTS

Ocular Hypertension

Rat eyes were subjected to unilateral elevated IOP via hypertonic saline injections into the limbal venous plexus. Within 3 days of injection, ipsilateral eyes from vehicle-treated animals demonstrated significant increases in IOP that continued to increase for 10 to 14 days, plateauing between 23 and 25 mm Hg (Fig. 2A). In vehicle-treated animals, cumulative IOPs over the course of the 28-day study showed that injected eyes were exposed to 633.5 ± 8.5 mm Hg hypertensive stress relative to a normotensive 365.8 ± 6.4 mm Hg in control eyes (Fig. 2B). Treatment with VPA did not significantly alter mean daily values or cumulative IOPs relative to vehicle-treated eyes. In the 28-day studies, one animal in each of the ocular-hypertensive groups did not achieve the minimum elevation of 7 mm Hg in IOP the hypertensive eye and was eliminated from further evaluation.

Retinal HDAC Activity

As shown in Figure 3, ocular-hypertensive stress in untreated animals resulted in a significant increase ($P < 0.05$) in class I HDAC activity as early as 1 week (13.3 ± 2.2%). This increase in class I HDAC activity remained significantly elevated (17.7 ± 1.9%) at 2 weeks. Class II HDAC activity was measured, but no significant changes were observed (data not shown). This

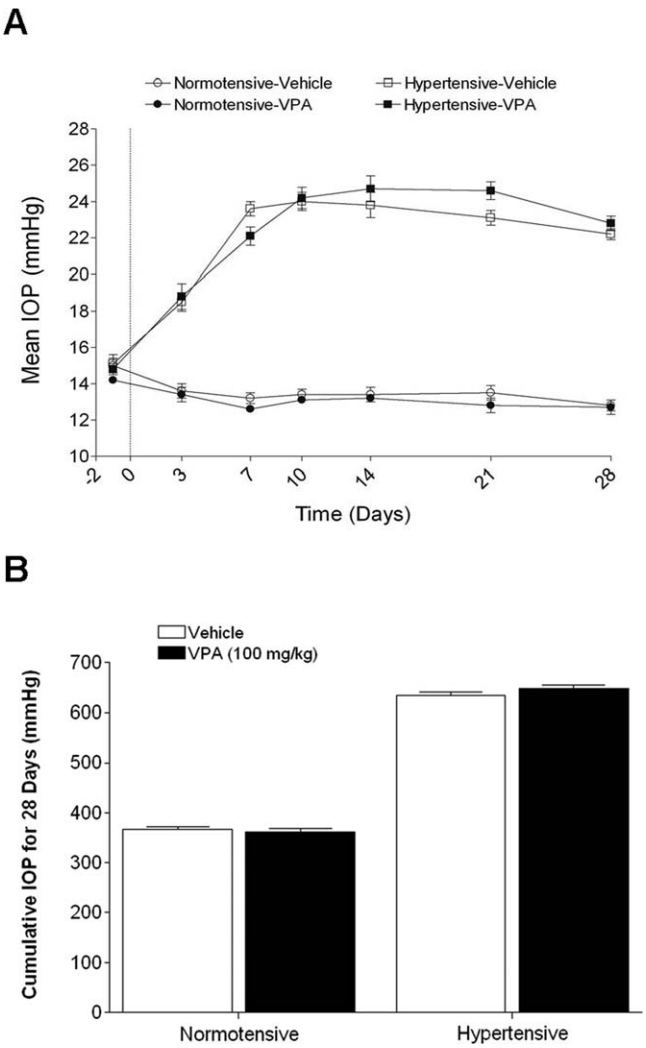

FIGURE 2. Effect of valproic acid on IOP. (A) Baseline IOPs were measured 1 day prior to ocular hypertension induction (day −1). On day 0, ocular hypertension was induced (*dashed line*) by injecting approximately 50 μL 2.0 M hypertonic saline unilaterally in VPA-treated and vehicle-treated Brown Norway rats. Contralateral eyes served as controls. On days 3 through 28, significant ($P < 0.001$; $n = 9$) differences in IOPs were observed between ocular-hypertensive eyes and normotensive eyes in both vehicle and VPA treatment groups. No significant difference in IOPs was observed when comparing IOPs between vehicle- and VPA-treated groups in corresponding eyes. (**B**) Mean cumulative IOPs, calculated by addition of all IOP measurements with extrapolation for days unmeasured. The net result is the area under the curve of (**A**). No significant differences were noted between control and VPA-treated groups in hypertensive or normotensive eyes ($n = 9$). VPA, valproic acid; IOP, intraocular pressure.

indicates that increase in HDAC activity is an early event following the induction of subchronic ocular hypertension.

Retinal Acetylation

As previous studies have presented evidence that acetyl-H3 levels provide a viable functional end point for monitoring the HDAC activity,[6,16,17] we examined the changes in retinal levels of acetyl-histone H3 following elevated IOP from untreated animals (Fig. 4). Contralateral eyes that did not receive hypertonic saline injection served as controls, and densitometry values were set at 100%. Although no significant change in acetyl-histone H3 levels was detected at 3 and 7 days following

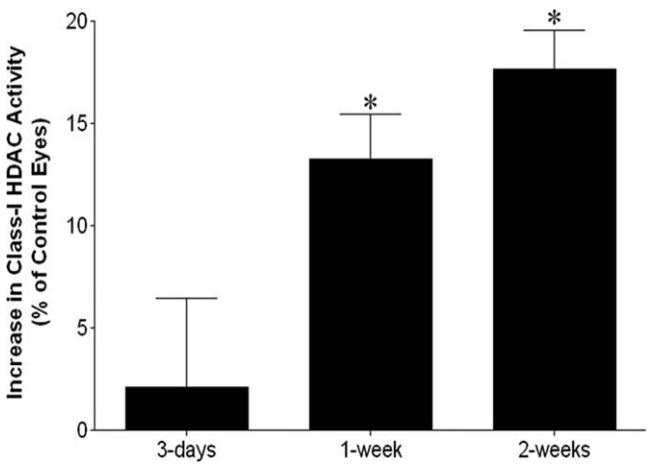

FIGURE 3. Effect of ocular hypertension on retinal class I HDAC enzymatic activity. Extent of HDAC activity was examined by fluorescent detection of aminomethoxy-cumarin (AMC) following cleavage from enzymatically deacetylated lysines at 3 days, 1 week, and 2 weeks following ocular-hypertensive injury. Significant increases in HDAC activity were observed at 1 week (13.3 ± 2.2%) and 2 weeks (17.7 ± 1.9%) post ocular hypertension initiation. HDAC activity was presented as the percent activity change in hypertensive eyes relative to the contralateral control eyes. $n = 4$; $^*P < 0.05$.

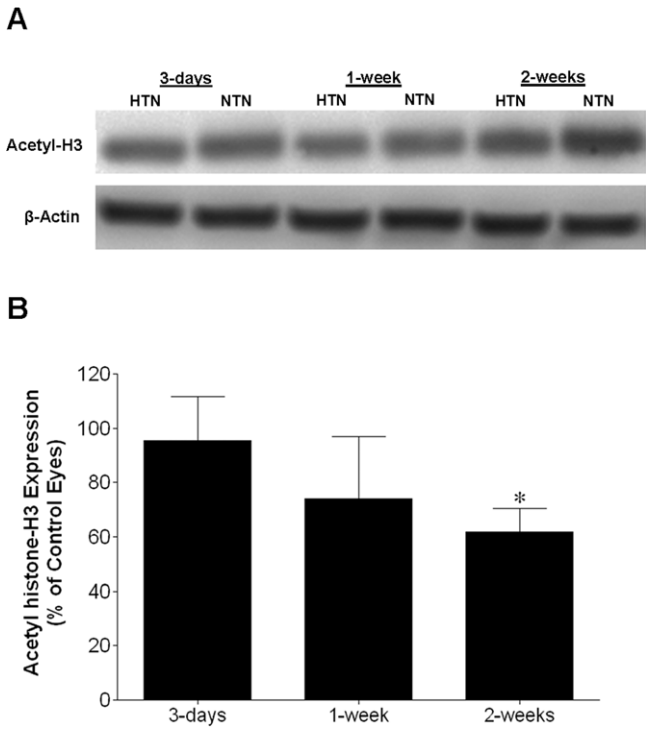

FIGURE 4. Effect of ocular hypertension on early changes in histone H3 acetylation. (**A**) Representative Western blot of retinal lysates for acetylated histone H3 normalized with β-actin. (**B**) Ratios of acetyl-histone H3 to β-actin were measured at 3 days, 1 week, and 2 weeks from the initiation of ocular hypertension. Ratio was expressed as a mean percentage of the hypertensive eyes relative to the control eyes (3 days, 95.5 ± 16.2%; 1 week, 74.2 ± 22.7%; 2 weeks, 61.9 ± 8.5%). $n = 4$; $^*P < 0.05$. Acetyl-H3, acetyl-histone H3; HTN, hypertensive eye; NTN, normotensive eye.

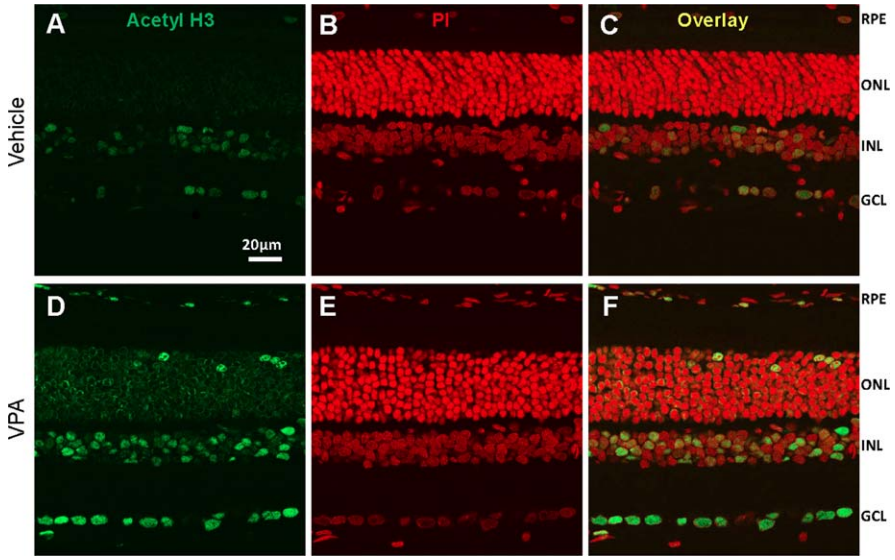

FIGURE 5. Effect of HDAC inhibition on retinal histone H3 acetylation. Animals were treated with vehicle ($n = 4$) or valproic acid (VPA; 100 mg/kg, i.p.) ($n = 4$) 2 hours prior to tissue analysis, and a representative acetyl-histone H3 immunohistochemical stain is shown. Immunohistochemical staining for (**A**) retina acetylated histone H3; (**B**) nuclei staining (*red*) and (**C**) overlay of image of (**A**) and (**B**) in vehicle-treated animals; (**D**) retina acetylated histone H3; (**E**) nuclei staining (*red*) and (**F**) overlay of image of (**D**) and (**E**) in VPA-treated animals. i.p., intraperitoneal.

elevation in IOP, a trend toward reduced acetylation was observed. However, following 2 weeks of ocular hypertension, acetyl-histone H3 levels were significantly reduced from control levels by 38.1 ± 8.5% ($P < 0.05$).

VPA Treatment

To assess if systemic administration of VPA can result in hyperacetylation of retinal proteins, rats were treated with VPA (100 mg/kg) or vehicle, and the levels of acetylated histone H3 in the retina were evaluated by immunohistochemistry 2 hours following intraperitoneal injection. Figure 5 shows immunohistochemical staining for acetyl-histone H3 in retinas from vehicle-treated normotensive animals. These retinas exhibited limited staining in the ganglion cell layer and in the inner nuclear layer. The systemic administration of VPA increased the staining for acetylated histone H3 in the ganglion cell layer and inner nuclear layer. In VPA-treated animals, acetylated histone H3 was also observed in outer nuclear layers and RPE.

The effects of vehicle and VPA treatment on pERG responses are summarized in Figure 6. In vehicle-treated animals, relative to contralateral control eyes, ocular hypertension induced a 29.1 ± 1.9% and 39.4 ± 2.0% reduction in pERGs at 2 weeks and 4 weeks, respectively. However, in animals treated with VPA, ocular-hypertensive eyes demonstrated significantly ($P < 0.05$) smaller reductions in pERG amplitudes at both 2 and 4 weeks when compared to vehicle-treated animals.

To measure morphologic changes induced by 28 days of ocular-hypertensive stress, RGC densities were evaluated by

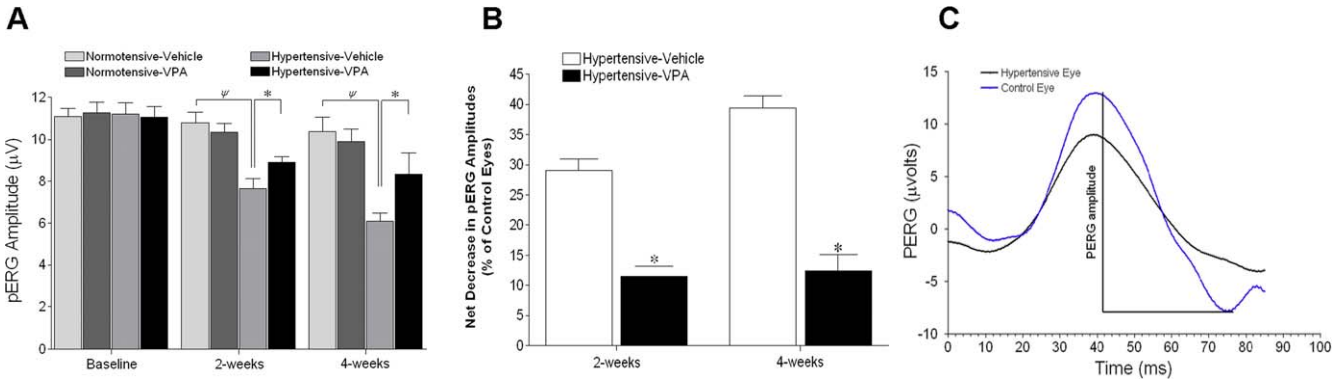

FIGURE 6. Effect of HDAC inhibition on functional neuroprotection using pattern electroretinography (pERG). Animals were treated with vehicle or valproic acid (VPA; 100 mg/kg; i.p.) twice daily on days 0 to 28, and resulting pERG amplitudes were recorded. (**A**) VPA administration showed significant preservation in raw pERG amplitudes compared to vehicle-treated counterparts at 2 weeks (8.9 ± 0.3 vs. 7.7 ± 0.5 μV) and 4 weeks (8.4 ± 1.0 vs. 6.1 ± 0.4 μV) post hypertension initiation. (**B**) Percentage reduction in pERG amplitudes of hypertensive eyes relative to normotensive contralateral control eyes (set at 0%). The decrease in pERG amplitudes of hypertensive eyes was calculated as a percentage of contralateral control eyes and adjusted by subtracting the absolute percentage change in amplitude of the contralateral control eyes from the respective baseline values. Vehicle-treated eyes demonstrated a 29.1 ± 1.9% and 39.4 ± 2.0% reduction at 2 weeks and 4 weeks, respectively. Eyes treated with VPA demonstrated significant preservation with 11.5 ± 1.7% and 12.4 ± 2.7% reduction at 2 weeks and 4 weeks, respectively ($n = 10$). (**C**) Representative pERG waveform from a control eye (*blue*) and ocular-hypertensive eye (*black*) at 4 weeks post injury initiation. *Asterisk* denotes significant difference between VPA-treated and vehicle-treated hypertensive groups. Data are expressed as mean ± SE. $^*P < 0.05$; $\psi P < 0.01$.

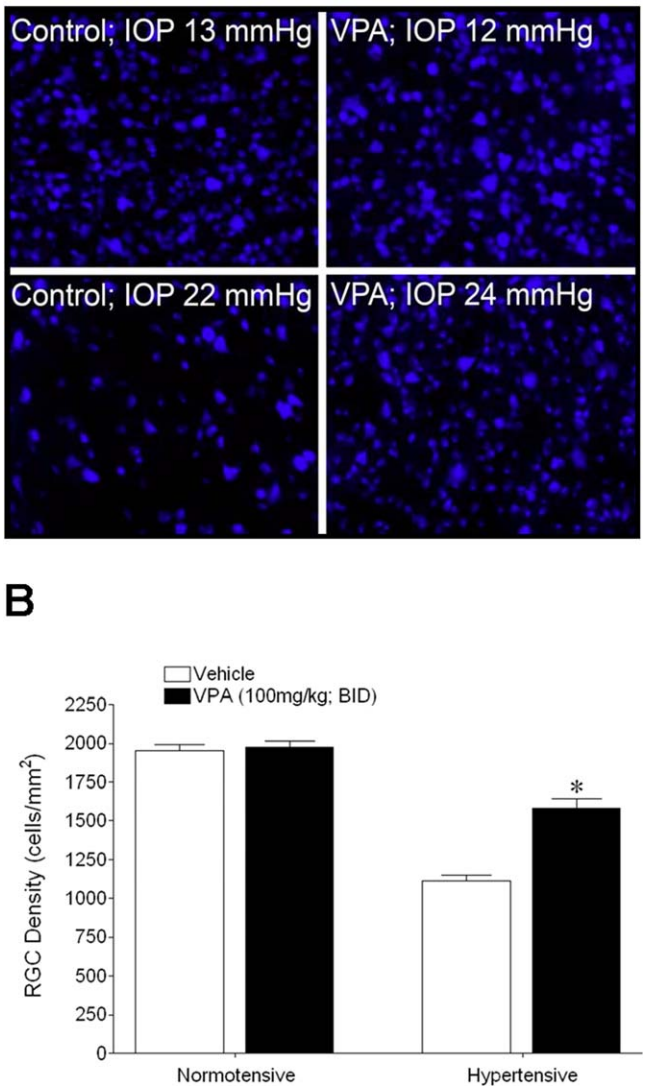

Figure 7. Effect of HDAC inhibition on RGC densities 5 days following injection of FluoroGold retrograde-labeling dye into the superior colliculi at day 28 of ocular hypertension. (**A**) Images of representative retinal flat mounts from all four groups with respective IOP measurements on day 28. (**B**) Vehicle-treated animals revealed a mean RGC density of 1951 ± 41 cells/mm^2 for contralateral control eyes and a significant decrease to 1114 ± 36 cells/mm^2 for hypertensive eyes. Animals treated with VPA demonstrated mean RGC densities of 1978 ± 38 and 1584 ± 60 cells/mm^2 in normotensive and hypertensive eyes, respectively. *Asterisks* denote significant increases in labeled RGCs in hypertensive eyes from rats receiving VPA compared to animals receiving vehicle treatment ($n = 10$). *$P < 0.05$. RGC, retinal ganglion cell; VPA, valproic acid; BID, twice daily.

retrograde labeling with hydroxystilbamidine (FluoroGold) dye (Fig. 7). In vehicle-treated animals, the mean RGC density for contralateral normotensive eyes was 1951 ± 41 cells/mm^2 and 1114 ± 36 cells/mm^2 in hypertensive eyes, as depicted in Figure 7B. In animals treated with VPA, mean RGC densities of 1978 ± 38 cells/mm^2 in contralateral control eyes and 1584 ± 60 cells/mm^2 in hypertensive eyes were measured (Fig. 7B). In VPA-treated animals, mean RGC density measurements were significantly larger when compared to corresponding measurements in hypertensive eyes of vehicle-treated animals. No significant difference was measured between contralateral control eyes of vehicle-treated and VPA-treated rats.

Discussion

Glaucoma is a disease characterized by visual field defects and optic nerve damage. Elevated IOP is a primary risk factor for glaucoma, and current therapies for controlling disease progression all target lowering IOP. However, it has been estimated that up to 50% of glaucomatous individuals do not exhibit elevated IOP.[2] As a result, other potential treatment strategies including enhancing vascular micronutrition of the retina and optic nerve, changing biochemical responses of the sclera and optic nerve head, and modification of glial cell responses have been postulated as effective glaucoma therapies.[3,18]

The reversible acetylation of nuclear histones and other cytoplasmic nonhistone proteins plays a critical role in gene expression, influencing the pathways undertaken by the cell in processes that vary from differentiation and repair to degeneration and cell death.[19] From a nuclear perspective, acetylation of histone tails promotes transcriptional activation through disruption of tight chromatin conformation, promoting chromatin relaxation that is generally more accessible to transcription factors, typically increasing transcriptional activation.[20] Conversely, deacetylation often accompanies the suppression of transcriptional activity by causing chromatin compaction. Since the discovery that p53 is a substrate for HDACs, there has been a rapidly growing list of proteins other than histones that undergo reversible acetylation.[21,22] As a result, these findings have established the importance of protein acetylation changes in the regulation of potentially a myriad of cellular processes.

Studies have provided evidence that HDAC inhibition can protect the retina from acute injury[5,9,10,23,24]; however, the use of HDAC inhibition in ocular hypertension models has received limited attention. A study by Pelzel et al.[25] utilized a DBA/2J mouse model and demonstrated beneficial effects of Trichostatin A treatment on RGC survival. Additionally, Biermann et al.[26] have shown the protective effects of VPA on RGCs in culture.The current study examined whether ocular hypertension alters acetylation status in the rat retina, and whether the modulation of acetylation can limit the course of ocular-hypertensive injury.

Studies in rodents have demonstrated that the retina expresses HDAC1, 2, 3, 4, 5, and 6,[7,27,28] and that HDAC1, 2, 3, and 6 can account for 98% of total HDAC activity.[7] In the current study, analysis of HDAC activity revealed that ocular hypertension induces a significant increase in class I HDAC activity within 1 week (Fig. 3), but no change in class II HDACs. This elevation in HDAC activity was associated with a subsequent decrease in histone H3 acetylation by week 2. This pattern of an increase in HDAC activity and resulting hypoacetylation of retinal protein has also been observed in models of ischemic retinal injury.[10] This recurrent theme in two distinct retinal injury models strongly argues in favor of an HDAC-dependent mechanism being involved in the initial sequelae of events that lead to retinal degeneration.

Valproic acid is a class I and II HDAC inhibitor. Like other HDAC inhibitors, VPA can have multiple actions that influence its in vivo efficacy. In addition to its actions as HDAC inhibitor, VPA has been shown to alter gamma-aminobutyric acid (GABA) synthesis and turnover and modulate the N-methyl-D-aspartate (NMDA) receptor activation, as well as altering the conductance of specific $Na^{\pm}$, Ca^{2+}, and $K^{\pm}$ channels.[29] Recent studies comparing retinal responses to two structurally distinct HDAC inhibitors, trichostatin-A and VPA, demonstrated that systemic

treatment with either agent produced similar increases in retinal protein acetylation and neuroprotection in an acute retinal ischemic model.[10] Taken together, these results support the idea that in vivo, VPA is an effective inhibitor of retinal HDAC and provide a rational basis for evaluating a VPA ocular-hypertensive model of retinal degeneration.

To investigate the role of protein acetylation in the development of ocular-hypertensive injury to the retina, we evaluated if VPA can alter the pathophysiological response to elevated IOP in a rat model of ocular hypertension. Our study utilized pattern electroretinography and retrograde FluoroGold labeling to assess RGC function and optic nerve axon integrity, respectively.[30,31] This study confirmed that in ocular-hypertensive rats, amplitudes of pERGs are significantly reduced (Fig. 6).[32] In addition, albeit not statistically significant, these results also revealed an age-related and VPA-related reduction in pERG amplitudes over the course of the study. To account for these changes, a net decrease in pERG amplitudes was calculated after normalization to contralateral control eyes and subtraction of crude amplitude loss at 2 weeks and 4 weeks from the respective baseline values; this is illustrated in Figure 6B. These results established that significant RGC functional loss occurs at 2 weeks after ocular hypertension initiation and continues to deteriorate at 4 weeks post injury initiation. In the presence of VPA, hypertensive eyes also lose function, but only during the initial 2 weeks and to a significantly lesser extent when compared to vehicle-treated counterparts (11.5% vs. 29.1% loss). After 2 weeks of ocular hypertension and IOP stabilization, HDAC inhibition preserves functioning RGCs as illustrated by the lack of further functional loss at 4 weeks. This information is important, as it illustrates that the majority of functional damage occurs within 2 weeks in the RGC injury response in our model of ocular-hypertensive injury.

In order to evaluate structural changes associated with RGC injury, retrograde FluoroGold labeling by injection of bilateral superior colliculi was performed. Figure 7 summarizes the mean RGC densities for all eyes; staining from individual retinal quadrants demonstrated that hypertensive eyes receiving HDAC inhibitor treatment had significantly greater staining of RGCs when compared to vehicle-treated eyes. Retinal temporal quadrants, and to a lesser extent nasal quadrants, had minor and insignificant decreases in RGC staining after sustained ocular hypertension when compared to superior and inferior retinal quadrants. This is consistent with the similar patterns of sectoral RGC loss in previous rodent glaucoma studies.[33] It has been reported that the uptake of FluoroGold by microglia cells occurs when RGCs degenerate.[14] The phagocytosis of this material can lead to labeling of glia. As a result, our cell counts may overestimate the number of RGCs in ocular-hypertensive eyes. Additionally, it is important to recognize that retrograde labeling measures RGC loss due to reduced axonal transport deficiency, axonal degeneration, and RGC degeneration.[34] However, combining these structural data with the functional pERG data, our results support the idea that HDAC inhibition promotes the survival of RGCs in ocular-hypertensive eyes.

In summary, this study supports the idea that the loss of RGCs in ocular-hypertensive eyes involves a relatively early increase in HDAC activity and the subsequent development of a hypoacetylated state in the retina. The administration of HDAC inhibitor, VPA, can protect RGCs from ocular-hypertensive stress. Together these data provide a rational basis for developing HDAC inhibitors for the treatment of optic neuropathies. Future studies need to investigate the cellular events that occur during the progression from ocular-hypertensive injury to deacetylation and apoptosis, and if these changes are due purely to a reduction in HDAC activity or if there is a concurrent increase in histone acetyltransferase enzyme activity.

Acknowledgments

The authors thank Luanna Bartholomew, PhD, for critical review of the manuscript.

Supported in part by National Institutes of Health, National Eye Institute Grant R01EY021368 (CEC), and an unrestricted grant to Storm Eye Institute, Medical University of South Carolina, from Research to Prevent Blindness, New York, New York, United States.

Disclosure: **O. Alsarraf**, None; **J. Fan**, None; **M. Dahrouj**, None; **C.J. Chou**, None; **P.W. Yates**, None; **C.E. Crosson**, None

References

1. Naskar R, Wissing M, Thanos S. Detection of early neuron degeneration and accompanying microglial responses in the retina of a rat model of glaucoma. *Invest Ophthalmol Vis Sci*. 2002;43:2962–2968.
2. Anderson DR. Normal-tension glaucoma (Low-tension glaucoma). *Indian J Ophthalmol*. 2011;59(suppl):S97–S101.
3. Quigley HA. Glaucoma. *Lancet*. 2011;377:1367–1377.
4. New M, Olzscha H, La Thangue NB. HDAC inhibitor-based therapies: can we interpret the code? *Mol Oncol*. 2012;6:637–656.
5. Biermann J, Grieshaber P, Goebel U, et al. Valproic acid-mediated neuroprotection and regeneration in injured retinal ganglion cells. *Invest Ophthalmol Vis Sci*. 2010;51:526–534.
6. Crosson CE, Mani SK, Husain S, Alsarraf O, Menick DR. Inhibition of histone deacetylase protects the retina from ischemic injury. *Invest Ophthalmol Vis Sci*. 2010;51:3639–3645.
7. Fan J, Alsarraf O, Dahrouj M, et al. Inhibition of HDAC2 protects the retina from ischemic injury. *Invest Ophthalmol Vis Sci*. 2013;54:4072–4080.
8. Petri S, Kiaei M, Kipiani K, et al. Additive neuroprotective effects of a histone deacetylase inhibitor and a catalytic antioxidant in a transgenic mouse model of amyotrophic lateral sclerosis. *Neurobiol Dis*. 2006;22:40–49.
9. Chen PS, Wang CC, Bortner CD, et al. Valproic acid and other histone deacetylase inhibitors induce microglial apoptosis and attenuate lipopolysaccharide-induced dopaminergic neurotoxicity. *Neuroscience*. 2007;149:203–212.
10. Alsarraf O, Fan J, Dahrouj M, Chou CJ, Menick DR, Crosson CE. Acetylation: a lysine modification with neuroprotective effects in ischemic retinal degeneration. *Exp Eye Res*. 2014;127:124–131.
11. Morrison JC, Moore CG, Deppmeier LM, Gold BG, Meshul CK, Johnson EC. A rat model of chronic pressure-induced optic nerve damage. *Exp Eye Res*. 1997;64:85–96.
12. McKinnon SJ, Lehman DM, Tahzib NG, et al. Baculoviral IAP repeat-containing-4 protects optic nerve axons in a rat glaucoma model. *Mol Ther*. 2002;5:780–787.
13. Sawada A, Neufeld AH. Confirmation of the rat model of chronic, moderately elevated intraocular pressure. *Exp Eye Res*. 1999;69:525–531.
14. Thanos S. The relationship of microglial cells to dying neurons during natural neuronal cell death and axotomy-induced degeneration of the rat retina. *Eur J Neurosci*. 1991;3:1189–1207.
15. Wegener D, Hildmann C, Riester D, Schwienhorst A. Improved fluorogenic histone deacetylase assay for high-throughput-screening applications. *Anal Biochem*. 2003;321:202–208.
16. Simonini MV, Camargo LM, Dong E, et al. The benzamide MS-275 is a potent, long-lasting brain region-selective inhibitor of histone deacetylases. *Proc Natl Acad Sci U S A*. 2006;103:1587–1592.

17. Zhang B, West EJ, Van KC, et al. HDAC inhibitor increases histone H3 acetylation and reduces microglia inflammatory response following traumatic brain injury in rats. *Brain Res*. 2008;1226:181–191.
18. Vrabec JP, Levin LA. The neurobiology of cell death in glaucoma. *Eye (Lond)*. 2007;21(suppl 1):S11–S14.
19. Haberland M, Montgomery RL, Olson EN. The many roles of histone deacetylases in development and physiology: implications for disease and therapy. *Nat Rev Genet*. 2009;10:32–42.
20. Chuang DM, Leng Y, Marinova Z, Kim HJ, Chiu CT. Multiple roles of HDAC inhibition in neurodegenerative conditions. *Trends Neurosci*. 2009;32:591–601.
21. Minucci S, Pelicci PG. Histone deacetylase inhibitors and the promise of epigenetic (and more) treatments for cancer. *Nat Rev Cancer*. 2006;6:38–51.
22. Yang XJ, Gregoire S. Class II histone deacetylases: from sequence to function, regulation, and clinical implication. *Mol Cell Biol*. 2005;25:2873–2884.
23. Chindasub P, Lindsey JD, Duong-Polk K, Leung CK, Weinreb RN. Inhibition of histone deacetylases 1 and 3 protects injured retinal ganglion cells. *Invest Ophthalmol Vis Sci*. 2013;54:96–102.
24. Pelzel HR, Schlamp CL, Nickells RW. Histone H4 deacetylation plays a critical role in early gene silencing during neuronal apoptosis. *BMC Neurosci*. 2010;11:62.
25. Pelzel HR, Schlamp CL, Waclawski M, Shaw MK, Nickells RW. Silencing of Fem1cR3 gene expression in the DBA/2J mouse precedes retinal ganglion cell death and is associated with histone deacetylase activity. *Invest Ophthalmol Vis Sci*. 2012; 53:1428–1435.
26. Biermann J, Boyle J, Pielen A, Lagreze WA. Histone deacetylase inhibitors sodium butyrate and valproic acid delay spontaneous cell death in purified rat retinal ganglion cells. *Mol Vis*. 2011;17:395–403.
27. Chen B, Cepko CL. Requirement of histone deacetylase activity for the expression of critical photoreceptor genes. *BMC Dev Biol*. 2007;7:78.
28. Schwechter BR, Millet LE, Levin LA. Histone deacetylase inhibition-mediated differentiation of RGC-5 cells and interaction with survival. *Invest Ophthalmol Vis Sci*. 2007;48:2845–2857.
29. Chateauvieux S, Morceau F, Dicato M, Diederich M. Molecular and therapeutic potential and toxicity of valproic acid. *J Biomed Biotechnol*. 2010;2010:1–18.
30. Holder GE. Pattern electroretinography (PERG) and an integrated approach to visual pathway diagnosis. *Prog Retin Eye Res*. 2001;20:531–561.
31. Husain S, Abdul Y, Crosson CE. Preservation of retina ganglion cell function by morphine in a chronic ocular-hypertensive rat model. *Invest Ophthalmol Vis Sci*. 2012;53:4289–4298.
32. Wanger P, Persson HE. Pattern-reversal electroretinograms in unilateral glaucoma. *Invest Ophthalmol Vis Sci*. 1983;24:749–753.
33. Perez de Lara MJ, Santano C, Guzman-Aranguez A, et al. Assessment of inner retina dysfunction and progressive ganglion cell loss in a mouse model of glaucoma. *Exp Eye Res*. 2014;122:40–49.
34. Badea TC, Williams J, Smallwood P, Shi M, Motajo O, Nathans J. Combinatorial expression of Brn3 transcription factors in somatosensory neurons: genetic and morphologic analysis. *J Neurosci*. 2012;32:995–1007.

Investigative Ophthalmology & Visual Science